Research Article

Green Synthesis Methods of CoFe$_2$O$_4$ and Ag-CoFe$_2$O$_4$ Nanoparticles Using Hibiscus Extracts and Their Antimicrobial Potential

Dana Gingasu,[1] Ioana Mindru,[1] Luminita Patron,[1] Jose Maria Calderon-Moreno,[1] Oana Catalina Mocioiu,[1] Silviu Preda,[1] Nicolae Stanica,[1] Sultana Nita,[2] Nicoleta Dobre,[2] Marcela Popa,[3] Gratiela Gradisteanu,[3] and Mariana Carmen Chifiriuc[3]

[1]*Ilie Murgulescu Institute of Physical Chemistry, Romanian Academy, 202 Splaiul Independentei, 060021 Bucharest, Romania*
[2]*National Institute for Chemical Pharmaceutical Research and Development, 112 Calea Vitan, 031299 Bucharest, Romania*
[3]*Microbiology Department, Faculty of Biology, University of Bucharest and Life, Environmental and Earth Sciences Division, Research Institute of the University of Bucharest (ICUB), 91-95 Splaiul Independentei, Bucharest, Romania*

Correspondence should be addressed to Ioana Mindru; imandru@yahoo.com

The cobalt ferrite (CoFe$_2$O$_4$) and silver-cobalt ferrite (Ag-CoFe$_2$O$_4$) nanoparticles were obtained through self-combustion and wet ferritization methods using aqueous extracts of *Hibiscus rosa-sinensis* flower and leaf. X-ray diffraction, scanning electron microscopy, Fourier transform infrared spectroscopy, and magnetic measurements were used for the characterization of the obtained oxide powders. The antimicrobial activity of the cobalt ferrite and silver-cobalt ferrite nanoparticles against Gram-positive and Gram-negative bacteria, as well as fungal strains, was investigated by qualitative and quantitative assays. The most active proved to be the Ag-CoFe$_2$O$_4$ nanoparticles, particularly those obtained through self-combustion using hibiscus leaf extract, which exhibited very low minimal inhibitory concentration values (0.031–0.062 mg/mL) against all tested microbial strains, suggesting their potential for the development of novel antimicrobial agents.

1. Introduction

Magnetic spinel ferrite nanoparticles have attracted an incredible attention over the past two decades, due to their improved properties over those exhibited by the "classic" materials with grains size >10 μm. The combination of their unique composition and the microstructure leads to a high potential for different applications, such as magnetic recording, magnetic energy storage, catalysis, biomedicine, and waste water treatment [1–7].

Among the spinel ferrites family, one of the most interesting is the inverse spinel cobalt ferrite (CoFe$_2$O$_4$) with great physical and chemical stability, having large anisotropy and saturation magnetization, as well as tunable coercivity [4], properties recommending it as a suitable candidate for biomedical applications [8, 9]. Recent studies revealed the antimicrobial activity of the cobalt ferrite nanoparticles on pathogenic and multidrug resistant bacterial strains [1].

On the other hand, cobalt ferrite acquires improved properties when combined with noble metals, like Ag or Au. Taking into account the inherent antimicrobial properties of Ag, it is expected that the addition of Ag to CoFe$_2$O$_4$ will enhance its antimicrobial activity [10–13].

It is well known that the synthesis method has a crucial influence on the composition, structure, and morphology and, implicitly, on the properties of the magnetic ferrite nanoparticles.

For this reason, chemists, physicists, and material scientists are focusing their researches to obtain nanoparticles with controllable size and morphology. Considerable efforts

have been made to develop wet chemical strategies especially those belonging to the soft chemistry—"chimie douce"—which correspond to these requirements.

The *"chimie douce"* (soft chemistry) is considered "the birth of the molecular engineering of nanomaterials" [14]. The concept of "chimie douce" was introduced by Livage [15–17]. All the methods belonging to the "chimie douce" are based on molecular precursors that allow a homogeneous distribution of chemical species at the molecular level. The precursor-polynuclear multimetallic compounds are capable of giving nanostructured ferrites by thermal decomposition or *in situ* decomposition processes [18].

The goal of today is to develop those synthesis strategies for nanomaterials which are eco-friendly, simple, and clean to "reduce or eliminate the use or the generation of hazardous substances in the design, manufacture and application of chemical products" [19]. The ideal synthesis strategy is the combination of the methods of soft chemistry and the green chemistry.

The green chemistry draws its inspiration from nature through plants, yeast, fungi, and bacteria. Integration of green chemistry principles is a key issue in the nanoscience research [20].

The use of plant extracts from leaves, flowers, roots, or seeds offers the possibility of preparing nanostructured magnetic ferrites *via* several chemical pathways using benign reagents thus reducing the risk of hazardous substances [21–24].

The plant extracts contain and can therefore release a variety of metabolites including carbohydrates, polysaccharides, phenols, amino acids, and vitamins, which can act as capping agents, reducing agents, and stabilizing and/or chelating agents for "capturing" the metal ions; they can also play a fuel role.

The use of plant extracts in the synthesis can influence the size, the shape, and the morphology of the nanoparticles. They generate nanoparticles with high dispersity, high stability, and narrow size distribution [23, 24].

Nowadays, a variety of plant extracts such as *Aloe vera* leaves, ginger roots, and *Hibiscus rosa-sinensis* flower/leaf are used to obtain metal oxides and mixed oxide nanoparticles [22–25].

An overview of the literature showed that *Hibiscus rosa-sinensis* flower/leaf extracts were often used to obtain Au and Ag nanoparticles [20, 26, 27], ZnO, and CeO_2 nanoparticles [28, 29].

In 2015, Manikandan et al. published the first study on the synthesis of spinel copper ferrite ($CuFe_2O_4$) using hibiscus flower extract [30].

Hibiscus rosa-sinensis has been used as a medicinal herb in native medicine, to cure many diseases. Its antibacterial activity is known for more than 50 years [20, 31–33]. The chemical composition of this plant includes organic and phenolic acids such as citric, malic, succinic, lactic, gallic, hibiscus, and homogentisic acids. Flavonoids such as quercetin, luteolin, gossypetin, and their glycosides are also present. Anthocyanins are responsible for the bright colour of the flowers. The chemical composition varies with the species, origin, age, and colour. The total phenolic compounds and

flavonoids are responsible for the antioxidant and antimicrobial activity [29, 34–36].

This work has the following goals: (i) the synthesis of cobalt ferrite nanoparticles ($CoFe_2O_4$) by self-combustion and wet ferritization methods using an aqueous extract *Hibiscus rosa-sinensis* flower/leaf, respectively; (ii) the synthesis of silver-cobalt ferrite nanoparticles ($Ag-CoFe_2O_4$) by self-combustion method using aqueous extracts hibiscus flower/leaf, respectively; (iii) the investigation of the antimicrobial activity of $CoFe_2O_4$ and $Ag-CoFe_2O_4$ nanoparticles against Gram-positive, Gram-negative, and fungal strains.

2. Experimental

2.1. Reagents. The iron nitrate ($Fe(NO_3)_3 \cdot 9H_2O$), the cobalt nitrate ($Co(NO_3)_2 \cdot 6H_2O$), and silver nitrate ($AgNO_3$) were of reagent quality (Merck). Hibiscus flowers/leaves were from local market.

2.2. Preparation of the Hibiscus Extracts

2.2.1. Preparation of Hibiscus Flower Extract. 5 g of dried flowers was placed in 100 mL distilled water under stirring. The mixture was boiled for 15 min. The bright red extract (pH = 2) was then cooled at room temperature and filtered.

2.2.2. Preparation of Hibiscus Leaf Extract. 5 g of fresh leaves was cut and was placed in 100 mL distilled water under continuous stirring. The mixture was boiled for 45 min. until the colour of the aqueous solution became yellow green (pH = 6). The extract was cooled at room temperature and filtered.

2.3. Synthesis of Cobalt Ferrites

2.3.1. The Self-Combustion Process. The metal nitrates ($2Fe^{3+}$: $1Co^{2+}$) were added slowly under stirring to the aqueous extract of *Hibiscus rosa-sinensis* flower. The obtained solution was concentrated until a gel was formed. This gel was placed on a heater at 250–300°C. Initially, the gel melted and, then, decomposed spontaneously by self-ignition, leaving behind voluminous foam (**H1**). This self-combustion reaction is a redox process in which the polyphenols from the hibiscus flower extract act as reducing agent. The magnetic foam was annealed at 800°C/1 h to improve the degree of crystallization of cobalt ferrite (**H1-800**).

2.3.2. The Wet Ferritization Reaction. The metal nitrates ($2Fe^{3+}$: $1Co^{2+}$) were added under stirring to the aqueous extract of *Hibiscus rosa-sinensis* leaf and the pH was raised to 10 by adding NH_4OH 25%. A dark brown precipitate was separated. The suspension was maintained at 80°C/4 h. After four hours, the precipitate became magnetic. It was filtered and dried (**H6**) on phosphorous pentoxide. A thermal treatment at 800°C for 1 h led to a well crystallized cobalt ferrite (**H6-800**).

2.4. Synthesis of $Ag-CoFe_2O_4$ Nanoparticles through Self-Combustion Method. Silver-cobalt ferrites have been obtained by the same procedure as for the $CoFe_2O_4$, described

above, using metal nitrates in a $2Fe^{3+} : 0.8Co^{2+} : 0.2Ag^+$ ratio and hibiscus flower/leaf extract (**H10/H11**). In order to improve the degree of crystallization, a thermal treatment at 800°C/1 h was required (**H10-800/H11-800**).

2.5. Characterization Techniques. A quantitative reversed-phase high-performance liquid chromatographic (RP-HPLC) method with DAD detection has been developed for the separation and the quantification of the flavonoids and phenolic acids in hibiscus flower/leaf extracts. The method is a direct procedure for simultaneous quantification of ten phenolic compounds: caffeic acid, rutin, rosmarinic acid, quercetin, kaempferol, gallic acid, homogentisic acid, pyrogallol, 2,5-dihydroxybenzoic acid, and 3,4-dihydroxybenzoic acid (250 mm × 4.6 mm × 5 μm, C18 column; mobile phase 30%–70% methanol gradient in 0.3 g/L solution of phosphoric acid adjusted to pH = 2.5). Fourier transform infrared spectroscopy (FTIR) spectra were recorded on KBr pellets, between $4000 \, cm^{-1}$ and $350 \, cm^{-1}$, with a sensitivity of $4 \, cm^{-1}$. The Nicolet 6700 apparatus with OMNIC soft was used for characterization. Powder X-ray diffraction patterns were recorded using Rigaku's Ultima IV multipurpose diffraction system. The diffractometer was set in parallel beam geometry, using Cu Kα radiation (λ = 1.5406 Å), CBO optics, and graphite monochromator and operated at 40 kV and 30 mA, 0.02° step size, and 1° min^{-1} scan speed. Phase identification was performed using Rigaku's PDXL software, connected to ICDD PDF-2 database. The lattice constants were refined using Whole Powder Pattern Fitting (WPPF) and crystallite size was calculated by Williamson-Hall method. The microstructure of the oxidic powders was studied by scanning electron microscopy (SEM) in a FEI Quanta 3D FEG apparatus operating at 5 kV, using secondary electrons (SE) and back-scattered electrons (BSE) micrographs, and equipped with an energy dispersive X-ray (EDX) spectrometer for elemental analysis measurements. The magnetic measurements were performed at room temperature on a Lake Shore's fully integrated Vibrating Sample Magnetometer (VSM) system 7404. In the interpretation of magnetic data the following were used: hysteresis curve (ferromagnetic phase)

$$M_T(H) = \frac{2M_{FM}^S}{\pi} a \tan\left[\frac{H \pm H_C}{H_C} \tan\left(\frac{\pi S}{2}\right)\right] + \chi_{paramag} H \quad (1)$$

and Langevin function (superparamagnetic phase)

$$M_T(H) = N_g \overline{\mu}\left[\coth\left(\frac{H}{T}\frac{\overline{\mu}}{k_B}\right) - \left(\frac{H}{T}\frac{\overline{\mu}}{k_B}\right)^{-1}\right] + \chi_{paramag} H. \quad (2)$$

Taking into account that, at high field, the magnetization increased almost linearly with external field in the hysteresis loops, the presence of a paramagnetic phase was considered and a supplementary term $\chi_{paramag} H$ was added.

M_{FM}^S and $M_{SP}^S = N_g \overline{\mu}$ are the saturation magnetization for the ferromagnetic (FM) and superparamagnetic (SP) components.

S is the squareness of the ferromagnetic loop, that is, the ratio of the remanent magnetization, M_R to M_{FM}^S.

H_C is the coercivity of the hysteresis loop.

$\overline{\mu}$ is the average moment per grain.

N_g is the number of grains (or nanoparticles)/cm^3 in the superparamagnetic component.

χ_g is the magnetic susceptibility per gram, for paramagnetic component.

2.6. Antimicrobial Activity Assays. The antimicrobial activity of the obtained compounds was assayed on Gram-negative (*Escherichia coli* ATCC 8739 and *Pseudomonas aeruginosa* ATCC 27853) and Gram-positive (*Staphylococcus aureus* ATCC 6538, *Enterococcus faecalis* ATCC 29212, *Staphylococcus saprophyticus* ATCC 15305, and *Bacillus subtilis* ATCC 6633) bacterial and fungal strains (*Candida albicans* ATCC 26790). Microbial suspensions of $1.5 \times 108 \, CFU \, mL^{-1}$ (0.5 McFarland density) obtained from 15 to 18 h bacterial cultures developed on solid media were used. The compounds were suspended in dimethyl sulfoxide (DMSO) to prepare a stock solution of $10 \, mg/mL^{-1}$ concentration. The qualitative screening was performed by an adapted disk diffusion method. In this purpose, Petri dishes with Mueller Hinton medium were seeded with bacterial inoculum as for the classical antibiotic susceptibility testing (Kirby-Bauer method); subsequently, 5 μL of the stock solution was spotted at 30 mm distance. The plates were left at room temperature for 20–30 min and then incubated at 37°C for 24 h. The positive results were read as the occurrence of an inhibition zone of microbial growth around the disk. The quantitative assay of the antimicrobial activity was performed by liquid medium microdilution method in 96 multiwell plates. Twofold serial dilutions of the compounds solutions (ranging between 1 mg and 0.002 mg·mL^{-1}) were performed in a 200 μL volume of broth, and each was well seeded with 50 μL microbial inoculum. Positive controls (wells containing culture medium seeded with the microbial inoculum) were used. The influence of the DMSO solvent was also quantified in a series of wells containing DMSO, diluted accordingly with the dilution scheme. The plates were incubated for 24 h at 37°C, and the minimal inhibitory concentration (MIC) values were considered as the lowest concentration of the tested compound that inhibited the growth of the microbial overnight cultures, as compared to the positive control, revealed by a decreased value of absorbance at 600 nm (Apollo LB 911 ELISA reader).

3. Results and Discussion

In this study, *Hibiscus rosa-sinensis* flower/leaf extracts have been used as gelling, reducing/chelating agent.
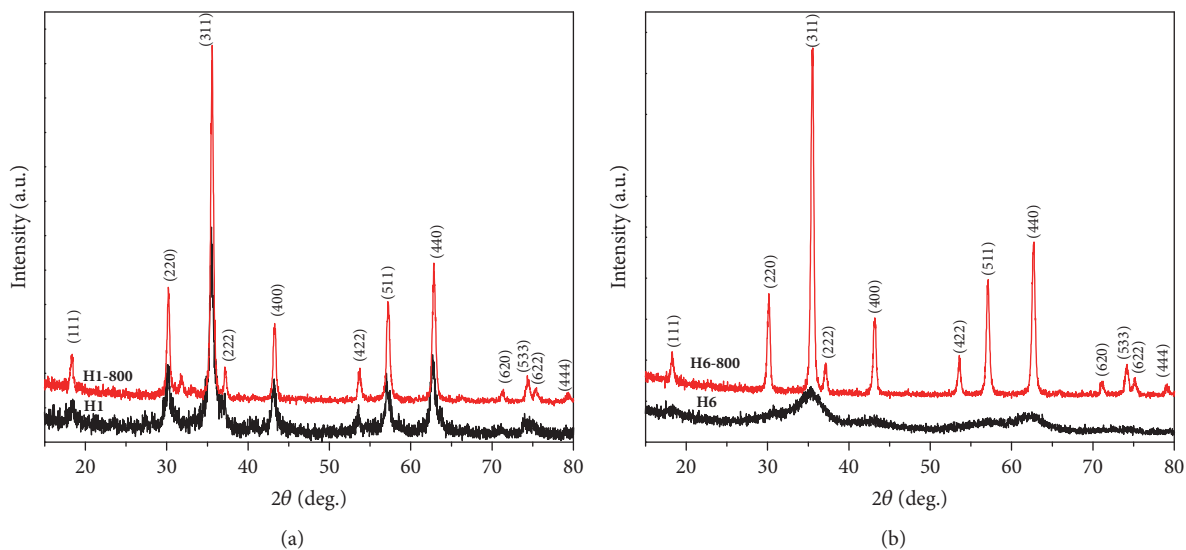
FIGURE 1: X-ray diffraction of the cobalt ferrites obtained by (a) self-combustion using hibiscus flower extract and (b) wet ferritization using hibiscus leaf extract.
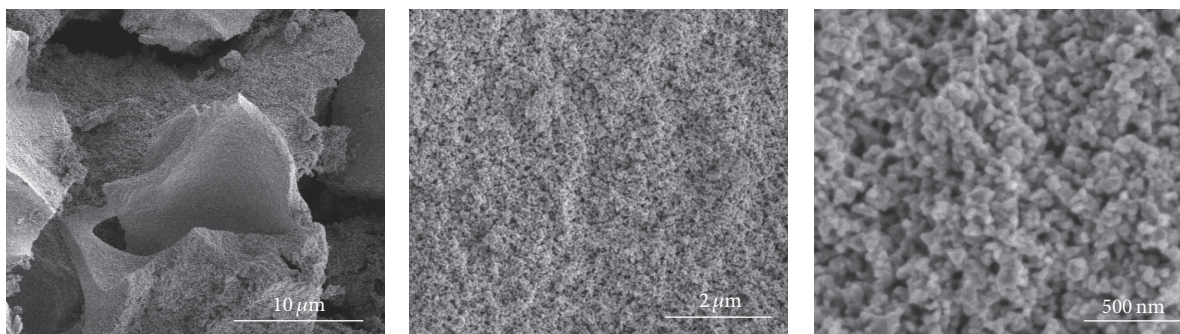

FIGURE 2: SEM micrographs of sample **H1-800** obtained through self-combustion method using hibiscus flower extract, at different magnifications.

The high-performance liquid chromatographic (HPLC) analyses of the aqueous extracts (Table 1) were in good agreement with the literature [33–37].

The $CoFe_2O_4$ and $Ag-CoFe_2O_4$ nanoparticles obtained by self-combustion and wet ferritization methods using flower and leaf extracts of hibiscus (Scheme 1), respectively, were characterized by XRD, SEM, FTIR, and magnetic measurements.

3.1. Characterization of $CoFe_2O_4$ Nanoparticles. The formation of the cobalt ferrite was confirmed by XRD patterns. Figure 1(a) shows the XRD patterns recorded for sample **H1** obtained through self-combustion method using hibiscus flower extract and for this sample calcined at 800°C/1 h, respectively (**H1-800**). XRD patterns indicate the formation of the $CoFe_2O_4$ cubic spinel structure (space group Fd3m, ICDD 022-1086). The lattice parameters were $a = 8.3839$ Å (for **H1**) and $a = 8.3626$ Å (**H1-800**) and in good agreement with the literature [38, 39]. The crystallites sizes were 10 nm for **H1** and 18 nm for **H1-800**.

Figure 1(b) showed the XRD patterns recorded for $CoFe_2O_4$ prepared through wet ferritization process. For

sample **H6**, the presence of characteristic peaks of cobalt ferrite confirmed that the phase of spinel cobalt ferrite was formed. A well crystallized $CoFe_2O_4$ was obtained after a treatment at 800°C/1 h; the lattice parameter was 8.3847 Å and the average crystallite size was 18.8 nm (**H6-800**).

SEM measurements of sample **H1-800** (Figure 2) show the formation of porous complex shape agglomerates with nanograined structure. Particle sizes and interparticle pores of ~30 nm are somewhat higher than crystallite sizes determined from XRD; the difference is attributed to early sintering of the nanocrystallites into secondary, nanosized agglomerates, leading to the formation of porous agglomerates.

SEM measurements of sample **H6**, obtained by the wet ferritization method, show the formation of agglomerates (Figure 3(a)) with a very fine nanograined structure (Figure 3(b)). The ill-defined contour of the grains (Figure 3(b)) is attributed to the incomplete crystallization and presence of remaining carbon from hibiscus leaf extract in the precipitate obtained through wet ferritization at room temperature. EDX spectroscopy elemental analysis detects the presence of C (4 wt%) (Figure 3(c)) and Si, P, and S as minor elements (<1 wt%); these are all elements present in the hibiscus leaf
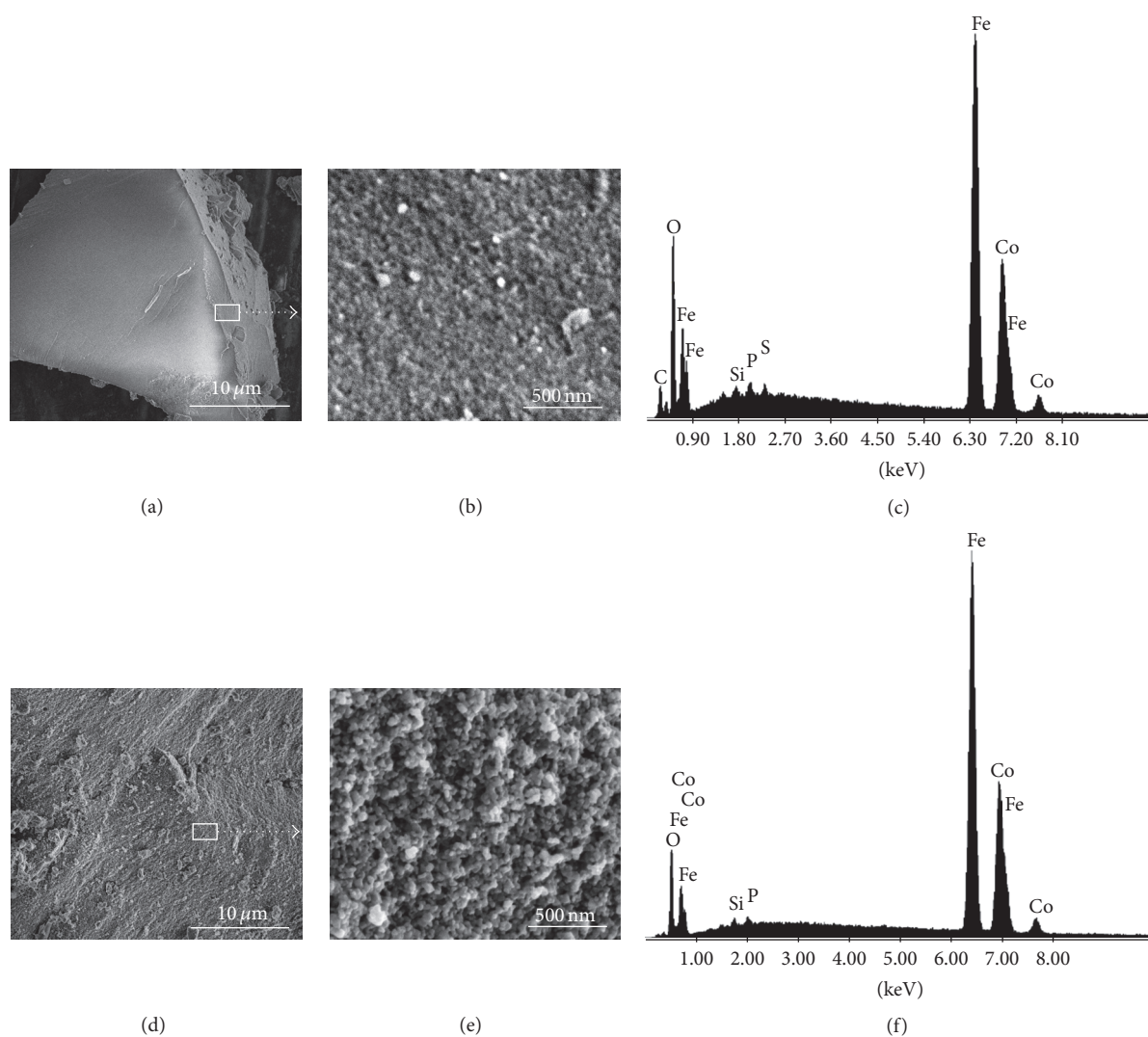
(a)

(b)

(c)

(d)

(e)

(f)

FIGURE 3: SEM micrographs and EDX spectra of the samples obtained through wet ferritization method using hibiscus leaf extract: (a–c) **H6** and (d–f) **H6-800**.

TABLE 1: Chemical composition of hibiscus flower/leaf extracts.

Flavonoid compounds/sample	Hibiscus flower extract		Hibiscus leaf extract	
	Retention time (min.)	Amount (mg/100 mL)	Retention time (min.)	Amount (mg/100 mL)
Caffeic acid	6.28	0.46	—	—
Rutin	—	—	12.2	0.304
Rosmarinic acid	—	—	—	—
Quercetin	—	—	22.95	0.187
Kaempferol	—	—	—	—
Gallic acid	2.87	0.850	2.99	0.297
Homogentisic acid	3.29	3.150	—	—
Pyrogallol	3.53	1031.737	3.54	4.753
3,4-Dihydroxybenzoic acid	4.04	0.767	4.1	2.995
2,5-Dihydroxybenzoic acid	6.22	6.734	—	—
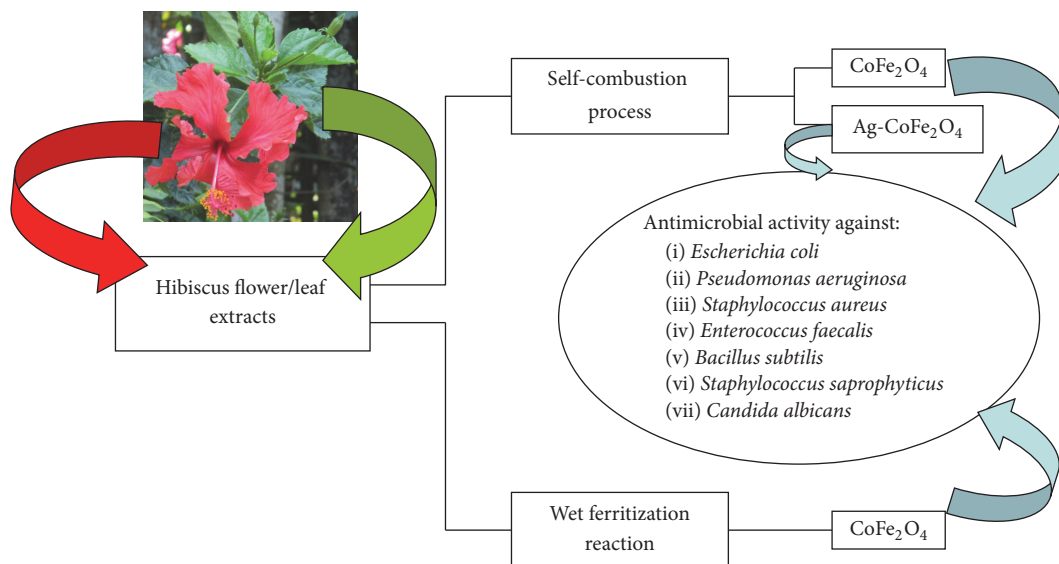
SCHEME 1: A general representation of the synthesis of $CoFe_2O_4$/Ag-$CoFe_2O_4$ nanoparticles and antimicrobial activity.

extract, the major component (~95 wt%) being the elements of $CoFe_2O_4$ nanocrystallites. SEM measurements of sample **H6-800**, after thermal treatment (Figures 3(d) and 3(e)), show fine-grained agglomerates with well-defined nanocrystallites and primary particle sizes of ~20 nm, in agreement with crystallite sizes determined from XRD measurements. EDX spectroscopy elemental analysis detects the elements of $CoFe_2O_4$ (>99 wt%) and the presence of Si and P as minor elements (<0.5 wt%), while C and S were not detected.

The FTIR spectra of all $CoFe_2O_4$ samples and those of hibiscus flower and leaf extracts are recorded in the 4000–350 cm^{-1} range.

In Table 2 the main peaks of infrared (FTIR) spectra for all samples analyzed in this work are listed. The assignment of bands is in good agreement with the literature data [18, 26, 31, 38].

The spectra of hibiscus flower and leaf extracts show main bands of O-H in water, C-H in CH_2 and in the phenyl ring, and symmetric and asymmetric vibrations of C-O and C=O bonds in COO$^-$ groups. In the spectrum of hibiscus flower extract supplementary bands of phenols at 2942 cm^{-1}, 1797 cm^{-1}, 1747 cm^{-1}, 1220 cm^{-1}, and 952 cm^{-1} are present. In this spectrum, there are also two bands of OH at 3564 cm^{-1} and 3271 cm^{-1} characteristic of water and phenols.

In sample **H1** obtained by self-combustion wide bands characteristic of the formation of cobalt ferrite at 653 cm^{-1} and 583 cm^{-1} were observed. The high carboxyl group bands were also present. It is very interesting to note that, even, after the thermal treatment, the bands characteristic of vibration of phenyl and carboxylate anions from the flower extract are present in the spectrum of **H1**. After thermal treatment, the bands of cobalt ferrite increased and they were shifted to lower wavenumbers. The bands of the spinel are well-defined in the range 370–800 cm^{-1}: ν_1 at 587 cm^{-1} assigned to the stretching vibration of Fe-O bond in the Td sites and ν_2 at

383 cm^{-1} assigned to the stretching vibration of Fe-O bond in the Oh sites.

The FTIR spectrum of sample **H6** evidenced two bands characteristic of the vibrations of νOH (1635 cm^{-1}) and carboxylate anions (1384 cm^{-1}) suggesting the formation of the bonds between the components of hibiscus leaf extract and the metal ions. This spectrum, also, showed the presence of strong bands at 591 cm^{-1} and 423 cm^{-1} characteristic of $CoFe_2O_4$, confirming the formation of the spinel ferrite by wet ferritization.

In the FTIR spectrum of sample obtained by wet ferritization (**H6**) the bands of cobalt ferrite are higher and better separated than in the spectrum of the sample obtained by self-combustion (**H1**); the bands of carboxylic groups are higher in FT-IR spectrum of **H1**. After thermal treatment at 800°C, the bands of cobalt ferrite increased in both cases.

The magnetization of $CoFe_2O_4$ samples was performed at room temperature. Experimental magnetic data was fitted with the hysteresis curve for ferromagnetic phase and Langevin function for superparamagnetic phase [40–42]. Figure 4 showed the magnetization (M) as function of the applied field (H).

The absence of the coercivity in the M-H curve (Figure 4(c)) for the $CoFe_2O_4$ particles obtained through wet ferritization method using hibiscus leaf extract (**H6**) indicated the superparamagnetic nature of the particles. The saturation magnetization (M_s) for the cobalt ferrite obtained by self-combustion method (**H1**) was found to be 25.94 emu/g and remanence (M_r) was 10.24 emu/g, while for **H1-800** the same parameters were 37.19 emu/g and 15.99 emu/g, respectively.

For the $CoFe_2O_4$ prepared by wet ferritization (**H6**), the saturation magnetization was 4.86 emu/g. The values of the saturation magnetization and remanence of cobalt ferrite, after the heat treatment (sample **H6-800**), were found to be 69.68 emu/g and 19.51 emu/g, respectively.

Table 2: The characteristic bands of the hibiscus flower/leaf extracts, $CoFe_2O_4$ and Ag-$CoFe_2O_4$ samples.

Hibiscus flower extract	H1	H1-800	H10	H10-800	Hibiscus leaf extract	H6	H6-800	H11	H11-800	Assignment
3564 vs,	3387 sh	—	3422 m	3422 m	3420 vs	3338 vs	3406 w	3420 m	3447 m	νOH in water
3271 vs	3177 vs	3058 w	—	—	—	—	—	—	—	νOH in phenols
2942 m	—	—	—	—	—	—	—	—	—	νCH in phenols
—	—	—	2927 w	2927 w	2930 m	2920 m	2917 w	2924 w	2924 w	νCH$_2$ asym
—	—	—	2850 w	2850 w	2847 m	2850 m	2854 w	2847 w	2847 w	νCH$_2$ sym
2622 m	—	—	—	—	—	—	—	—	—	νOH
2537 m	—	—	—	—	—	—	—	—	—	νOH
1797 vs	—	—	—	—	—	—	—	—	—	γCH in phenols
1747 vs	—	—	—	—	—	—	—	—	—	γCH in phenols
1636 vs	—	1622 w	1635 w	1635 w	1636 vs	1635 s	1623 w	1630 w	—	νOH in water
1605 sh	1601 vs	—			1647 sh	1647 sh	—	—	—	νCOO$^-$ asym
1417 m	1384 vs	1456 sh / 1394 m	1414 s / 1384 s	1463 m / 1384 m	1384 vs	1384 m	—	1384 s	—	νCOO$^-$ sym
1270 m	—	—		—	1258 m	—	—	—	—	νC-O-C asym
1220 s	1228 sh	—			—	—	—	—	—	νC-OH and δCH in phenols
1186 s	—	—	—	—	1120 s	—	—	—	—	νC-OH
1093 s	—	1110 w	1110 w	1114 m	1042 s	1046 m	1051 w	1098 m	1098 m	νC-O-C sym
1065 s	1077 m	—	—	1049 m	—	—	985 w	—	986 w	νC-O-C sym
952 m	963 w	940 w	—	—	—	—	—	—	—	δCH in phenols
914 w	914 w	—	—	—	899 m	—	—	831 w	844 w	γCH ring vibration
862 m	847 w	832 w	859 w	863 w	809 m	—	—	—	—	γCH ring vibration
776 w	790 w	—			699 m	—	—	—	—	γCH ring vibration
717 m	—	—	—	—	617 m / 537 m	—	—	—	—	γCH ring vibration
—	653 m	587 vs	571 m	591 vs	—	591 s	578 vs	560 s	587 vs	νM-O in spinel
	583 m	383 s	382 m	386 s		423 s	375 vs	379 s	375 vs	

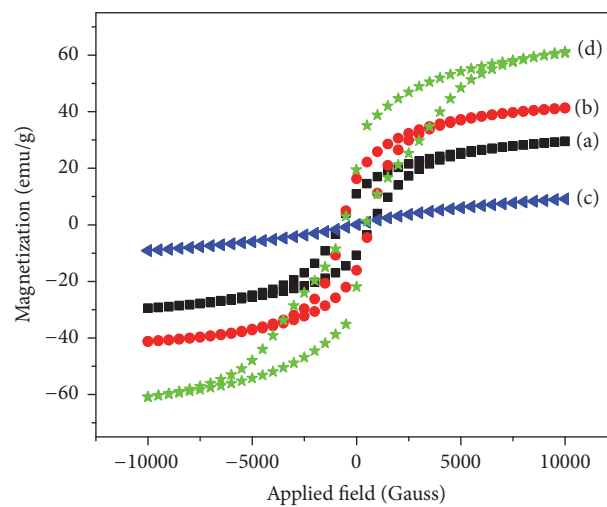vs = very strong, s = strong, m = medium, w = weak, and sh = shoulder.

Figure 4: Magnetization versus applied field of the cobalt ferrites: (a) **H1**, (b) **H1-800**, (c) **H6**, and (d) **H6-800**.
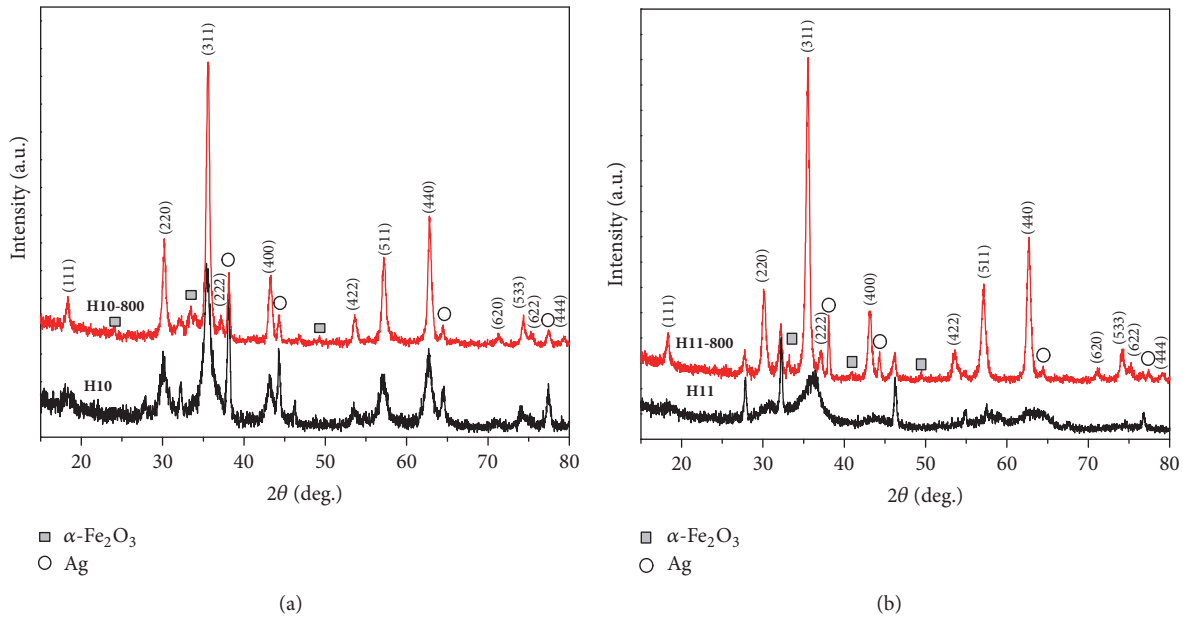
FIGURE 5: X-ray diffraction of the Ag-cobalt ferrite nanoparticles obtained by self-combustion using (a) hibiscus flower extract and (b) hibiscus leaf extract.

3.2. Characterization of Ag-CoFe$_2$O$_4$ Nanoparticles. The XRD patterns of the silver-cobalt ferrites (Ag-CoFe$_2$O$_4$) obtained through self-propagating using hibiscus flower/leave extract (**H10/H11**) and Ag-CoFe$_2$O$_4$ calcined at 800°C/1 h (**H10-800/H11-800**) are presented in Figure 5.

The XRD patterns of the samples **H10** and **H11** showed the formation of CoFe$_2$O$_4$ (ICDD 022–1086) and Ag nanoparticles (space group Fm-3m; ICDD 004–0783). The examination of the patterns also indicated the presence of some traces of α-Fe$_2$O$_3$ and unidentified peaks. Heating treatment at 800°C/1 h led to well crystallized Ag-CoFe$_2$O$_4$ nanoparticles. The lattice parameter *a* of cobalt ferrite ranged between 8.364 Å for **H10-800** and 8.3775 Å for **H11-800**; the average crystallite size of cobalt ferrites was 15.8 nm/14.8 nm (for **H10-800/H11-800**), respectively.

SEM measurements of samples **H10** and **H11** (Figure 6), obtained through self-combustion using hibiscus flower and leaf extracts, respectively, show the formation of powder agglomerates with very fine nanograined structure. In both samples primary particle sizes are below 10 nm, indicating that the presence of Ag inhibits crystallite growth, but the aggregation state of primary crystallites varies significantly; in **H10** they form micron size aggregates (Figure 6(a)) with a porous crystalline framework (Figure 6(b) and inset) while in **H11** the primary nanocrystallites connect forming spheres (Figure 6(e)), with diameters around 200 nm, the spheres themselves forming larger agglomerates (Figure 6(d)). EDX spectroscopy elemental analysis (Figures 6(c) and 6(f)) detects the presence of Ag together with P and S as minor elements (<0.5 wt%), the major component (>99 wt%) being the elements of CoFe$_2$O$_4$ nanocrystallites.

The formation of the cobalt ferrite was also evidenced through IR spectra of the samples **H10**, **H10-800**, **H11,** and **H11-800** recorded between 4000 cm^{-1} and 350 cm^{-1}.

The FTIR spectra of **H10** and **H10-800** present few differences. In the spectrum of sample **H10-800** the bands characteristic of COO$^-$ groups decreased and the C-O-C bands increased. This behaviour can be correlated with the decomposition of carboxylate anions. The bands characteristic of cobalt ferrite can be seen at 591 cm^{-1} and 386 cm^{-1}.

In the FTIR spectrum of **H11** sample, the cobalt ferrite bands are present. In the spectrum of **H11-800**, the decrease in intensity of bands characteristic of hydroxyl and carboxyl group bands and an increase in intensity of cobalt ferrite bands can be seen.

Comparative observation of the FTIR spectra of the samples treated at 800°C/1 h shows the decrease of carboxylate and hydroxyl anions bands in the case of sample **H11-800**.

The presence of Ag in samples improved the formation of spinel in the samples obtained by self-combustion.

Figure 7 shows the magnetization versus field (*M-H* curves) for Ag-CoFe$_2$O$_4$ nanoparticles obtained by self-combustion using hibiscus flower/leaf extracts (samples **H10** and **H11**) and Ag-CoFe$_2$O$_4$ annealed at 800°C/1 h (samples **H10-800** and **H11-800**). The absence of the remanence (M_r) and the coercivity (H_c) on the *M-H* curve for sample **H11** (Figure 7(b)) evidences a superparamagnetic behaviour. The saturation magnetization (M_s) for **H11** is 2.72 emu/g. For the silver-cobalt ferrite obtained through self-combustion using hibiscus flower extract (**H10**) the values of saturation magnetization and remanence are 27.06 emu/g and 6.46 emu/g, respectively. It can be observed that M_s value of Ag-CoFe$_2$O$_4$ obtained by self-combustion using hibiscus leaf flower extract
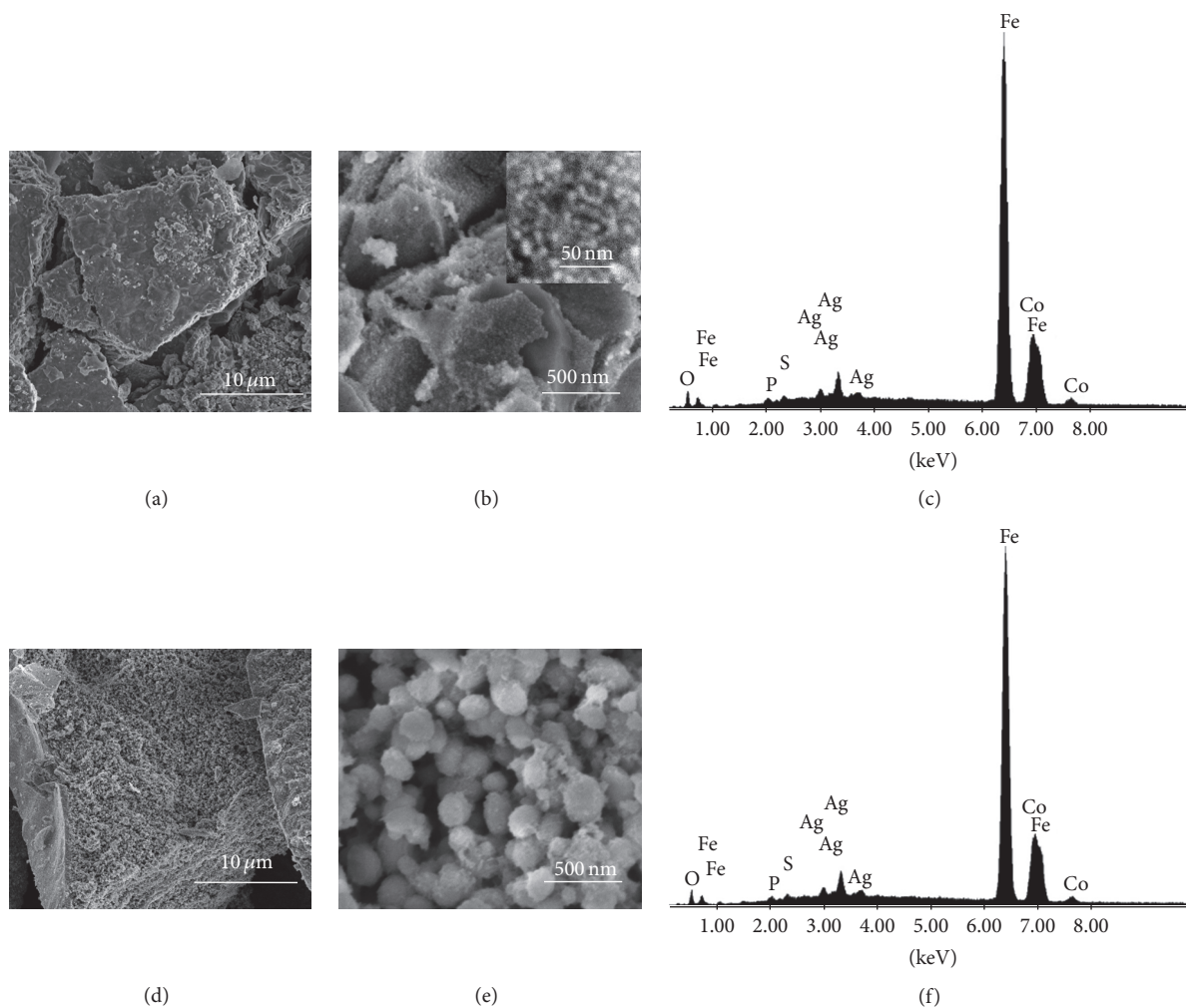
FIGURE 6: SEM micrographs and EDX spectra of the samples obtained through self-combustion using (a–c) hibiscus flower extract (**H10**) and (d–f) hibiscus leaf extract (**H11**).

increased after heat treatment (sample **H11-800**), due to the increase in particle size ($M_s = 35.69$ emu/g).

3.3. Antimicrobial Activity. Until now, there are only few reports in the literature concerning the antimicrobial activity of Ag-CoFe$_2$O$_4$ [43].

During the present study, new Ag-CoFe$_2$O$_4$ nanoparticles together with CoFe$_2$O$_4$ nanoparticles have been tested for their antimicrobial activity, using Gram-negative and Gram-positive bacteria, as well as fungal strains.

The qualitative method used for the screening of the antimicrobial activity of the tested nanoparticles (Table 3) indicated that **H10** followed by **H11** and **H1** proved to be the most active, inducing the total inhibition of the microbial growth and the occurrence of growth inhibition zones with diameters ranging from 6 to 10 mm. The most susceptible strains were the Gram-positive *Enterococcus faecalis*, the Gram-negative *Escherichia coli,* and *Candida albicans* yeast strain.

Additionally, the **H10** nanoparticles induced the partial inhibition of the two *Staphylococcus sp.* tested strains, **H11** of

Pseudomonas aeruginosa and *Staphylococcus saprophyticus,* and **H1** of *Escherichia coli* and *Staphylococcus saprophyticus* strains.

The quantitative assay of the antimicrobial activity of the obtained nanoparticles confirmed the qualitative screening results, indicating **H10** the most active nanoparticles, exhibiting the lowest MIC values ranging from 0.031 to 0.062 mg/mL against all tested bacterial and yeast strains (Table 4). **H11** followed by **H6** and **H1** exhibited only a moderate antimicrobial activity with MIC values between 0.125 and >1 mg/mL (Table 4).

4. Conclusions

The CoFe$_2$O$_4$ and Ag-CoFe$_2$O$_4$ nanoparticles were obtained by wet ferritization and self-combustion methods using *Hibiscus rosa-sinensis* flower/leaf extracts. To the best of our knowledge, there are no literature data on the synthesis of CoFe$_2$O$_4$ using hibiscus extracts as chelating/gelling agent.

The as-prepared samples were characterized by various techniques. XRD analysis demonstrated that both methods
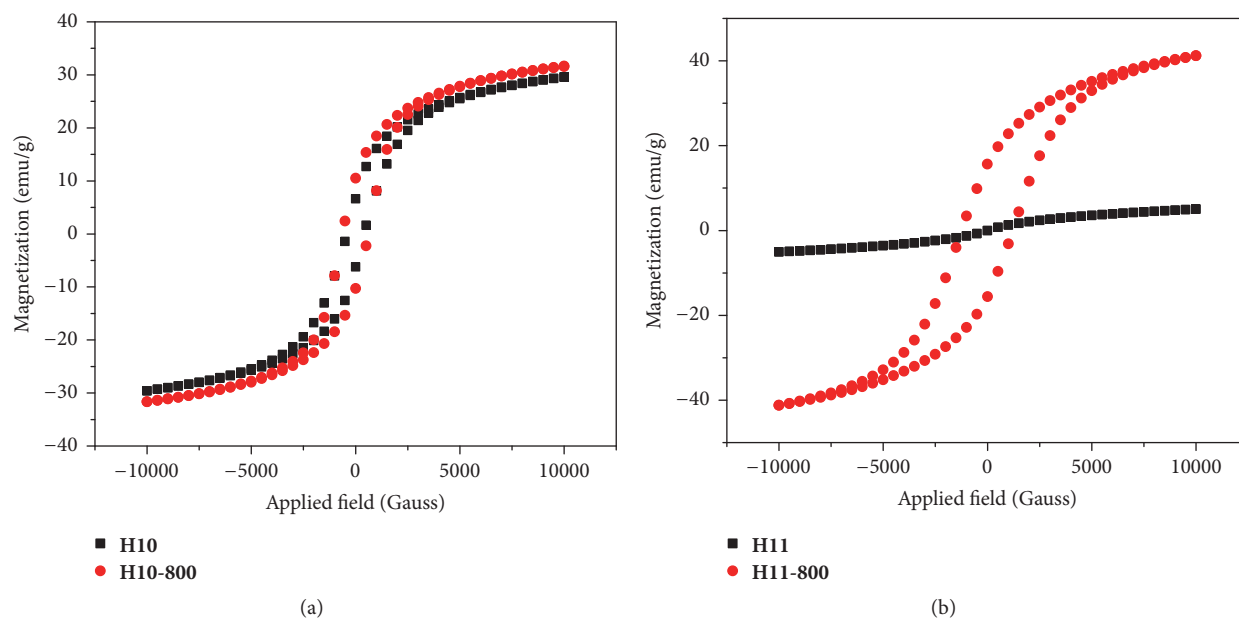
(a)

(b)

FIGURE 7: Magnetization versus applied field of the Ag-cobalt ferrite nanoparticles obtained by self-combustion using (a) hibiscus flower extract and (b) hibiscus leaf extract.

TABLE 3: Results of the qualitative screening of the antimicrobial activity of the tested samples expressed in mm of the growth inhibition zone diameter.

Microbial tested strains	H11	H6	H10	H1	Flower extract	Leaf extract	DMSO
Escherichia coli ATCC 8739	8*	0	8*	+/−**	0	0	+/−**
Pseudomonas aeruginosa ATCC 27853	+/−**	0	0	0	0	+/−**	0
Staphylococcus aureus ATCC 6538	0	0	+/−**	0	+/−**	0	0
Staphylococcus saprophyticus ATCC 15305	+/−**	+/−**	+/−**	+/−**	+/−**	+/−**	
Enterococcus faecalis ATCC 29212	7*	0	10*	8*	0	8*	0
Bacillus subtilis ATCC 6633	0	0	6*	8*	0	0	0
Candida albicans ATCC 26790	6*	0	6*	6*	0	0	0

Numbers (∗), diameter (mm) of the growth inhibition zone; +/− (∗∗), partial inhibition of the microbial growth; 0, absence of growth inhibition.

have led to the formation of $CoFe_2O_4/Ag$-$CoFe_2O_4$ with cubic spinel structure. XRD of the samples calcined at 800°C/1 h indicated the formation of the spinel-type $CoFe_2O_4$ with good crystallinity. The morphology of the obtained $CoFe_2O_4/Ag$-$CoFe_2O_4$ nanoparticles was investigated by SEM measurements. The EDX spectra evidenced the presence of Co, Fe, and Ag in the Ag-$CoFe_2O_4$ nanoparticles. The presence of C, Si, P, and S as minor elements was associated with the elemental content of the plant extracts. FTIR spectra sustained the formation of cobalt ferrite by both methods. The magnetic measurements revealed a superparamagnetic behaviour for samples **H6** and **H11**.

The antimicrobial activity assay indicated that the Ag-$CoFe_2O_4$ (**H10/H11**) nanoparticles exhibited an improved inhibitory effect against the bacterial and fungal tested strains, as compared to $CoFe_2O_4$ nanoparticles obtained by either of the two methods. The most active nanostructure was

represented by silver-cobalt ferrite (Ag-$CoFe_2O_4$) obtained through self-combustion using hibiscus leaf extract, exhibiting very low MIC values against a wide range of microbial strains including Gram-negative fermentative and nonfermentative bacilli, Gram-positive cocci, and bacilli, and yeast strains.

Competing Interests

The authors declare that there are no competing interests.

Acknowledgments

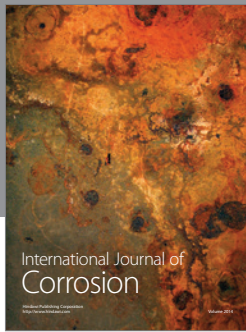TABLE 4: Results of the quantitative assay of the antimicrobial activity of the tested samples expressed in mg/mL.

Microbial tested strains	H11	H6	H10	H1	Leaf extract	Flower extract
Escherichia coli ATCC 8739	0.5**	>1***	0.062*	>1***	>1***	>1***
Pseudomonas aeruginosa ATCC 27853	0.25**	0.5**	0.031*	1***	>1***	1***
Staphylococcus aureus ATCC 6538	0.25**	0.5**	0.062*	>1***	>1***	>1***
Staphylococcus saprophyticus ATCC 15305	0.125**	0.25**	0.031*	0.5**	>1***	>1***
Enterococcus faecalis ATCC 29212	0.5**	1***	0.062*	>1***	1***	>1***
Bacillus subtilis ATCC 6633	0.25**	0.25**	0.062*	0.125**	1***	1***
Candida albicans ATCC 26790	0.25**	0.125**	0.062*	1***	>1***	1***

∗ denotes the good inhibitory activity with low MIC values; ∗∗ denotes the moderate antimicrobial activity with MIC values from 0.125 to 0.5 mg/mL; ∗ ∗ ∗ denotes the low antimicrobial activity with MIC values >0.5 mg/mL.

References

[1] A. Pathak and P. Pramanik, "Nano-particles of oxides through chemical methods," *Proceedings of the Indian National Science Academy*, vol. 67, no. 1, pp. 47–70, 2001.

[2] C. Wang and S. Sun, "Chemical synthesis of monodisperse magnetic nanoparticles," in *Handbook of Magnetism and Advanced Magnetic Materials*, John Wiley & Sons, 2007.

[3] D. S. Mathew and R.-S. Juang, "An overview of the structure and magnetism of spinel ferrite nanoparticles and their synthesis in microemulsions," *Chemical Engineering Journal*, vol. 129, no. 1–3, pp. 51–65, 2007.

[4] Z. Jia, D. Ren, and R. Zhu, "Synthesis, characterization and magnetic properties of CoFe$_2$O$_4$ nanorods," *Materials Letters*, vol. 66, no. 1, pp. 128–131, 2012.

[5] H. Wang, D. Liu, Y. Li, and Q. Duan, "Single-spinneret electrospinning fabrication of CoFe$_2$O$_4$ nanotubes as high-performance anode materials for lithium-ion batteries," *Materials Letters*, vol. 172, pp. 64–67, 2016.

[6] P. C. Morais, "Photoacoustic spectroscopy as a key technique in the investigation of nanosized magnetic particles for drug delivery systems," *Journal of Alloys and Compounds*, vol. 483, no. 1-2, pp. 544–548, 2009.

[7] S. Zhang, Y. Zhang, G. Bi et al., "Mussel-inspired polydopamine biopolymer decorated with magnetic nanoparticles for multiple pollutants removal," *Journal of Hazardous Materials*, vol. 270, pp. 27–34, 2014.

[8] S. Amiri and H. Shokrollahi, "The role of cobalt ferrite magnetic nanoparticles in medical science," *Materials Science and Engineering: C*, vol. 33, no. 1, pp. 1–8, 2013.

[9] N. Sanpo, J. Wang, and C. C. Berndt, "Influence of chelating agents on the microstructure and antibacterial property of cobalt ferrite nanopowders," *Journal of the Australian Ceramic Society*, vol. 49, no. 1, pp. 84–91, 2013.

[10] N. Sanpo, C. C. Berndt, C. Wen, and J. Wang, "Transition metal-substituted cobalt ferrite nanoparticles for biomedical applications," *Acta Biomaterialia*, vol. 9, no. 3, pp. 5830–5837, 2013.

[11] S. Velho-Pereira, A. Noronha, A. Mathias et al., "Antibacterial action of doped CoFe$_2$O$_4$ nanocrystals on multidrug resistant bacterial strains," *Materials Science and Engineering: C*, vol. 52, pp. 282–287, 2015.

[12] S. Xavier, H. Cleetus, P. J. Nimila, S. Thankachan, R. M. Sebastian, and E. M. Mohammed, "Structural and antibacterial properties of silver substituted cobalt ferrite nanoparticles," *Research Journal of Pharmaceutical, Biological and Chemical Sciences*, vol. 5, no. 5, pp. 364–371, 2014.

[13] R. Shukla, R. S. Ningthoujam, S. S. Umare et al., "Decrease of superparamagnetic fraction at room temperature in ultrafine CoFe$_2$O$_4$ particles by Ag doping," *Hyperfine Interactions*, vol. 184, no. 1, pp. 217–225, 2008.

[14] C. Sanchez, L. Rozes, F. Ribot et al., "'Chimie douce': a land of opportunities for the designed construction of functional inorganic and hybrid organic-inorganic nanomaterials," *Comptes Rendus Chimie*, vol. 13, no. 1-2, pp. 3–39, 2010.

[15] J. Livage, "Chimie douce: from shake-and-bake processing to wet chemistry," *New Journal of Chemistry*, vol. 25, no. 1, p. 1, 2001.

[16] M. Yoshimura and J. Livage, "Soft processing for advanced inorganic materials," *MRS Bulletin*, vol. 25, no. 9, pp. 12–13, 2000.

[17] D. Avnir, O. Lev, and J. Livage, "Recent bio-applications of sol-gel materials," *Journal of Materials Chemistry*, vol. 16, no. 11, pp. 1013–1030, 2006.

[18] I. Mindru, D. Gingasu, D. C. Culita, G. Marinescu, and L. Patron, "Design and synthesis of magnetic ferrites," in *Dekker Encyclopedia of Nanoscience and Nanotechnology*, S. E. Lyshevski, Ed., pp. 2176–2189, CRC Press, New York, NY, USA, 3rd edition, 2014.

[19] P. T. Anastas and J. C. Warner, *Green Chemistry: Theory and Practice*, Oxford University Press, New York, NY, USA, 1998.

[20] D. Philip, "Green synthesis of gold and silver nanoparticles using *Hibiscus rosa sinensis*," *Physica E: Low-Dimensional Systems and Nanostructures*, vol. 42, no. 5, pp. 1417–1424, 2010.

[21] A. Manikandan, R. Sridhar, S. Arul Antony, and S. Ramakrishna, "A simple aloe vera plant-extracted microwave and conventional combustion synthesis: morphological, optical, magnetic and catalytic properties of CoFe$_2$O$_4$ nanostructures," *Journal of Molecular Structure*, vol. 1076, pp. 188–200, 2014.

[22] S. Phumying, S. Labuayai, E. Swatsitang, V. Amornkitbamrung, and S. Maensiri, "Nanocrystalline spinel ferrite (MFe$_2$O$_4$, M = Ni, Co, Mn, Mg, Zn) powders prepared by a simple aloe vera plant-extracted solution hydrothermal route," *Materials Research Bulletin*, vol. 48, no. 6, pp. 2060–2065, 2013.

[23] P. Laokul, V. Amornkitbamrung, S. Seraphin, and S. Maensiri, "Characterization and magnetic properties of nanocrystalline CuFe$_2$O$_4$, NiFe$_2$O$_4$, ZnFe$_2$O$_4$ powders prepared by the Aloe vera extract solution," *Current Applied Physics*, vol. 11, no. 1, pp. 101–108, 2011.

[24] R. S. Varma, "Greener approach to nanomaterials and their sustainable applications," *Current Opinion in Chemical Engineering*, vol. 1, no. 2, pp. 123–128, 2012.

[25] P. Laokul and S. Maensiri, "Aloe vera solution synthesis and magnetic properties of Ni-Cu-Zn ferrite nanopowders," *Journal of Optoelectronics and Advanced Materials*, vol. 11, no. 6, pp. 857–862, 2009.

[26] K. C. Bhainsa and S. F. D'Souza, "Extracellular biosynthesis of silver nanoparticles using the fungus *Aspergillus fumigatus*," *Colloids and Surfaces B: Biointerfaces*, vol. 47, no. 2, pp. 160–164, 2006.

[27] S. Shabana, M. S. Muzamonil, and S. Parsana, "Silver nano scaffold formation by flowers of *Hibiscus rosa sinensis*," *International Journal of Herbal Medicine*, vol. 1, no. 2, pp. 169–174, 2013.

[28] A. Yasmin, K. Ramesh, and S. Rajeshkumar, "Optimization and stabilization of gold nanoparticles by using herbal plant extract with microwave heating," *Nano Convergence*, vol. 1, no. 1, article 12, 2014.

[29] N. Thovhogi, A. Diallo, A. Gurib-Fakim, and M. Maaza, "Nanoparticles green synthesis by *Hibiscus Sabdariffa* flower extract: main physical properties," *Journal of Alloys and Compounds*, vol. 647, pp. 392–396, 2015.

[30] A. Manikandan, M. Durka, and S. Arul Antony, "*Hibiscus rosa-sinensis* leaf extracted green methods, magneto-optical and catalytic properties of spinel $CuFe_2O_4$ nano- and microstructures," *Journal of Inorganic and Organometallic Polymers and Materials*, vol. 25, no. 5, pp. 1019–1031, 2015.

[31] Z. W. Atwan and F. Saiwan, "The antibacterial activity of cold aqueous and pigment of *Hibiscus rosa sinensis* extracts against gram positive and negative bacteria," *Basrah Journal of Veterinary Research*, vol. 10, no. 2, pp. 109–118, 2010.

[32] A. Kumar and A. Singh, "Review on *Hibiscus rosa sinensis*," *International Journal of Pharma and Bio Sciences*, vol. 3, pp. 534–538, 2012.

[33] Y. W. Mak, L. O. Chuah, R. Ahmad, and R. Bhat, "Antioxidant and antibacterial activities of hibiscus (*Hibiscus rosa-sinensis* L.) and Cassia (*Senna bicapsularis* L.) flower extracts," *Journal of King Saud University-Science*, vol. 25, no. 4, pp. 275–282, 2013.

[34] T. O. Alaga, M. O. Edema, A. O. Atayese, and M. Bankole, "Phytochemical and in vitro anti-bacterial properties of Hibiscus sabdariffa L (Roselle) juice," *Journal of Medicinal Plants Research*, vol. 8, no. 7, pp. 339–344, 2014.

[35] A. P. Obouayeba, D. N. Bernard, D. Sekou et al., "Phytochemical and antioxidant activity of Roselle (*Hibiscus sabdariffa* L) petal extracts," *Research Journal of Pharmaceutical, Biological and Chemical Sciences*, vol. 5, no. 2, pp. 1453–1465, 2014.

[36] A. Bhaskar, V. Nithya, and V. G. Vidhya, "Phytochemical screening and *in vitro* antioxidant activities of the ethanolic extract of *Hibiscus rosa-sinensis* L," *Annals of Biological Research*, vol. 2, no. 5, pp. 653–661, 2011.

[37] W. G. A. Al Shoosh, *Chemical composition of some Roselle (Hibiscus sabdariffa) genotypes [Ph.D. thesis]*, University of Khartoum, 1993.

[38] V. Kumar, A. Rana, M. S. Yadav, and R. P. Pant, "Size-induced effect on nano-crystalline $CoFe_2O_4$," *Journal of Magnetism and Magnetic Materials*, vol. 320, no. 11, pp. 1729–1734, 2008.

[39] R. M. Mohamed, M. M. Rashad, F. A. Haraz, and W. Sigmund, "Structure and magnetic properties of nanocrystalline cobalt ferrite powders synthesized using organic acid precursor method," *Journal of Magnetism and Magnetic Materials*, vol. 322, no. 14, pp. 2058–2064, 2010.

[40] M. B. Stearns and Y. Cheng, "Determination of para- and ferromagnetic components of magnetization and magnetoresistance of granular Co/Ag films," *Journal of Applied Physics*, vol. 75, no. 10, pp. 6894–6899, 1994.

[41] J. C. Cezar, M. Knobel, and H. C. N. Tolentino, "Magnetic properties of Cu-permalloy granular alloy," *Journal of Magnetism and Magnetic Materials*, vol. 226–230, pp. 1519–1521, 2001.

[42] M. Kuźmiński, A. Ślawska-Waniewska, H. K. Lachowicz, and M. Knobel, "The effect of particle size and surface-to-volume ratio distribution on giant magnetoresistance (GMR) in melt-spun Cu–Co alloys," *Journal of Magnetism and Magnetic Materials*, vol. 205, no. 1, pp. 7–13, 1999.

[43] M. Kooti, S. Saiahi, and H. Motamedi, "Fabrication of silver-coated cobalt ferrite nanocomposite and the study of its antibacterial activity," *Journal of Magnetism and Magnetic Materials*, vol. 333, pp. 138–143, 2013.